Catalysis Letters 58 (1999) 207–212

Entrapment of nanostructured palladium clusters in hydrophobic sol–gel materials

Manfred T. Reetz * and Markus Dugal

Max-Planck-Institut für Kohlenforschung, Kaiser-Wilhelm-Platz 1, D-45470 Mülheim an der Ruhr, Germany
E-mail: reetz@mpi-muelheim.mpg.de

Received 8 December 1998; accepted 25 February 1999

The fluoride-catalysed hydrolysis of mixtures of $CH_3Si(OCH_3)_3$ and $Mg(OC_2H_5)_2$ in the presence of preformed nanosized $R_4N^+Br^-$-stabilised Pd colloids results in the formation of micro/mesoporous hydrophobic sol–gel materials in which the Pd clusters are entrapped individually in the solid matrix. The materials are active catalysts in the hydrogenation of 1,5-cyclooctadiene.

Keywords: Pd colloids, cluster immobilisation, catalytic hydrogenation, methyl-silicates, sol–gel catalysts

1. Introduction

Nanosized transition metal colloids are of interest as potential catalysts in organic chemistry, as electrocatalysts in fuel cells and as components in nanoelectronics [1]. They are generally prepared by the reduction of transition metal salts in the presence of stabilisers such as special ligands, polymers or surfactants which prevent the undesired formation of insoluble metal powders. In most cases structural information concerning the role of the stabiliser is lacking, although it is generally assumed that the stabiliser surrounds the metal core [1]. A rare case in which this was proven concerns a study in which the combination of transmission electron microscopy (TEM) and scanning electron microscopy (STM) was used to elucidate the structural details of $R_4N^+Br^-$-stabilised palladium clusters [2].

The long-standing problem of size-selectivity in the synthesis of preformed colloids [3] has been solved in some cases [4,5],[1] although a general method is still not available. For genuine applications of such materials in catalysis, some form of immobilisation on the surface of solid supports such as SiO_2 or Al_2O_3 appears to be necessary [1,6]. However, pronounced advantages relative to classical methods based on impregnation/calcination/reduction of metal salts need to be demonstrated. Moreover, other strategies have emerged, including the fixation of metal clusters in the cages of zeolites [7]. In a novel alternative approach it was recently demonstrated that structurally discrete metal complexes such as $[Ag_3Ru_{10}C_2(CO)_{28}Cl]^{2-}$ can be adsorbed on the inner walls of the silicate-phase MCM-41, and that following thermolysis catalytically active materials are obtained in which bimetallic particles are aligned evenly in the channels [8]. The incorporation of phenanthroline-stabilised giant Pd clusters of the Moiseev–Schmid-type in the mesopores (and on the external surface) of MCM-41 is also possible, resulting in materials which catalyse CO oxidation [9]. Finally, the encapsulation of gold clusters in the micropores of xerogels and aerogels by sequential reduction of gold salts followed by sol–gel processing in an inverse micelle solution has been reported recently, although the question of catalytic properties was not addressed [10].

Our own goal was to entrap $R_4N^+X^-$-stabilised transition metal clusters, prepared size-selectively by an electrochemical procedure [5], in hydrophobic sol–gel materials produced by the hydrolysis of $CH_3Si(OCH_3)_3$ or $RSi(OCH_3)_3$ [11,12].[2] Previously, we had demonstrated that enzymes such as lipases can be encapsulated in similar amorphous materials, leading to heterogeneous biocatalysts which show dramatically enhanced stability, activity (factors of 5–100) and in some cases even stereoselectivity [13]. Although the reasons for such superior properties have not been elucidated unambiguously, it became clear that a hydrophobic environment in the pores of the gels, brought about by the presence of the non-hydrolysable methyl (or alkyl) groups on silicon, is essential, analogous entrapment by a traditional sol–gel process based on the hydrolysis of $Si(OCH_3)_4$ leading to materials which show almost no enzymatic activity ($<5\%$). Thereafter the concept of controlling hydrophobicity by the use of alkyl-modified sol–gel precursors was extended to catalytically active amorphous mixed metal oxides (e.g., Si/Ti) [14]. In this important study it was shown that activity and selectivity in peroxide-mediated oxidation reactions can be controlled by adjusting the surface polarity, a property that can be measured by determining the hydrophobicity index (relative adsorption of n-octane versus H_2O) [14,15].

---

* To whom correspondence should be addressed.

[1] $R_4N^+X^-$-stabilised metal colloids have been prepared previously, but not in a size-selective manner [1].

[2] We thank K. Wanninger for preliminary experiments (1994).

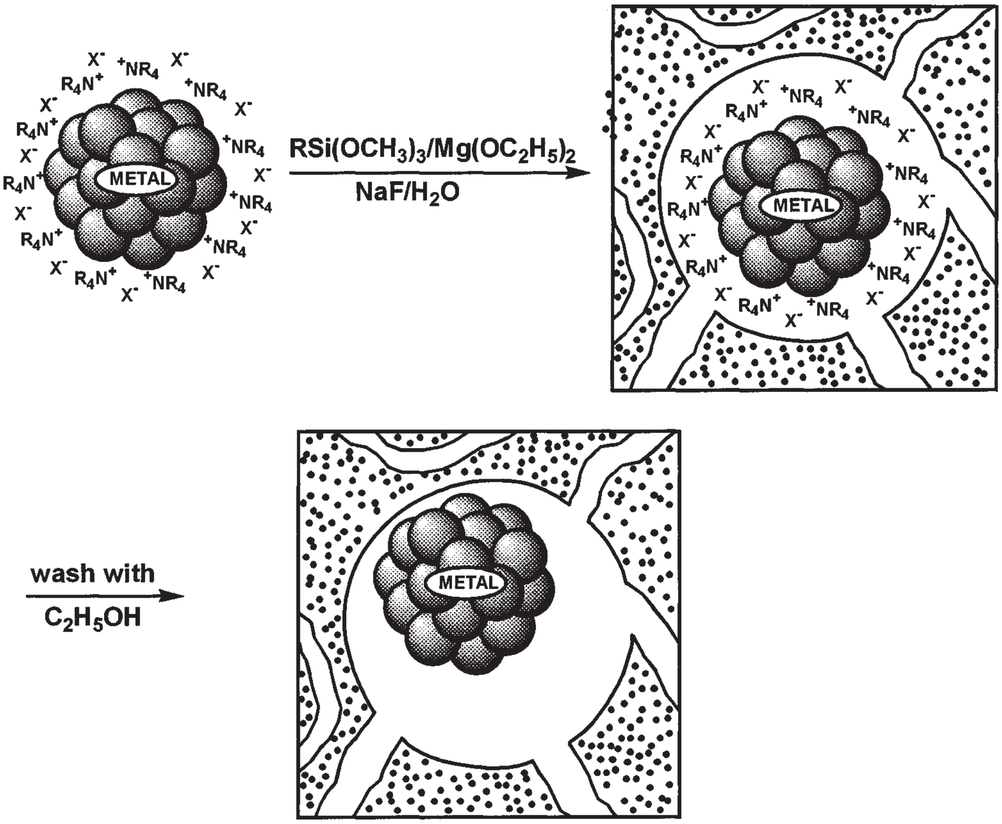

Figure 1. General scheme for the entrapment of preformed metal clusters in sol–gel materials.

The challenge in the present work was to find conditions under which the sol–gel process proceeds with encapsulation of individual metal clusters *and* formation of gels having optimal morphological properties such as sufficiently large pore sizes (volumes) and high surface area. At the outset it became clear that an additional feature is possible, namely the presence of a second metal oxide in the matrix brought about by copolymerisation of the corresponding metal alkoxide. Specifically, $Mg(OC_2H_5)_2$ was first considered, since it was known that MgO is a promoter in certain Pd-catalysed reactions [16]. In principle, the overall concept entails the control of several parameters important for potential catalysis: (1) Nature and size of the preformed mono- or bimetallic clusters; (2) degree of hydrophobicity in the matrix; (3) possibility of built-in promoters. Finally, it was anticipated that the stabiliser can be extracted following entrapment, leading to the fixation of “naked” Pd clusters in a type of “microreactor” (figure 1).

2. Experimental

2.1. Catalyst preparation

In a 50 ml polypropylene vessel a solution of Mg $(OC_2H_5)_2$ in absolute methanol (1.6 M) and $CH_3Si(OCH_3)_3$ were mixed before a solution of a $Pd/N(C_8H_{17})_4Br$ colloid [5] in THF (0.23 M) was added. After a short period of mixing (5–10 s) an aqueous NaF solution (8.5×10^{-4} M) and methanol were added ($R =$ water/alkoxide ratio $= 4.0$). The vessel was closed and vigorously shaken in a vortex mixer until gelation. The resulting homogeneous black gel was aged for 24 h at room temperature, then air-dried at 50 °C for 3–4 days and crushed in a mortar to obtain a greyish powder. The extraction of the stabiliser was carried out in a 50 ml round bottom flask with 35 ml ethanol under reflux conditions and magnetic stirring. After an extraction duration of 3 days the catalyst powder was isolated by centrifugation, thoroughly washed with ethanol and air-dried at 50 °C.

2.2. Catalyst characterisation

The specific surface areas and pore volumes were derived from N_2- and Ar-physisorption isotherms, which were obtained on a Sorptomatic 1990 (Fisons Instruments) at 77 and 87 K, respectively. CO-chemisorption measurements were carried out on a AMI 1 pulse chemisorption apparatus (Altamira Instruments). X-ray diffraction was executed on a Stoe STAD/2/PL powder diffractometer using a Cu $K\alpha_1$ source. Surface acidity was measured after adsorption of pyridine using FTIR spectroscopy in diffuse reflectance (DRIFTS) on a Bruker IFS 48 spectrometer equipped with a Harrick Drift unit (DRA) in combination with a high-vacuum chamber (HVC). High-resolution TEM micrographs were obtained by field emission transmission electron microscopy (Hitachi, HF 2000, 200 keV) coupled with EDX analysis.

Table 1
Characterisation of the Pd sol–gel catalysts and a commercial Pd/Al_2O_3 catalyst by physisorption and TEM.

Catalyst designation	Catalyst gel derived from	Specific surface area[a] (m^2/g)	Porosity	Specific pore volume[b] (cm^3/g)	Pd particle size[c] (nm)
I	$Si(OCH_3)_4$	590	micro–mesoporous	0.61	100–200
II	$CH_3Si(OCH_3)_3$	520	micro–mesoporous	0.41	100–200
III	$Si(OCH_3)_4$/ $(CH_3O)_3SiOAl(O$*sec*-$C_4H_9)_2$	10	non-porous	0.02	3.5
IV	$CH_3Si(OCH_3)_3/Mg(OC_2H_5)_2$ (1 : 1)	420	micro–mesoporous	0.16[d]	2.0
V	$CH_3Si(OCH_3)_3/Mg(OC_2H_5)_2$ (2 : 1)	420	micro–mesoporous	0.20[d]	2.0
VI	$CH_3Si(OCH_3)_3/Mg(OC_2H_5)_2$ (3 : 1)	375	micro–mesoporous	0.43	3.5
VII	$CH_3Si(OCH_3)_3/Mg(OC_2H_5)_2$ (3 : 1)	415	micro–mesoporous	0.40	2.0
VIII	$CH_3Si(OCH_3)_3/Mg(OC_2H_5)_2$ (5 : 1)	380	micro–mesoporous	0.20[d]	2.0
IX	$CH_3Si(OCH_3)_3/Mg(OC_2H_5)_2$ (7 : 1)	280	micro–mesoporous	1.03	2.0
X	Pd/Al_2O_3 (Degussa E 211 R/D)	370	mesoporous	1.41	3[e]

[a] Calculated from adsorption isotherms using the BET method (±10–20% uncertainty).
[b] Calculated from desorption isotherms using the Dollimore Heal method (±10–20% uncertainty).
[c] Mean Pd particle diameters derived from TEM micrographs.
[d] Calculated from adsorption isotherm using the Horvath–Kawazoe method due to a high micropore percentage.
[e] Broad particle size distribution from 1–5 nm.

2.3. Catalyst activity

Under a stream of argon a quantity of the Pd catalyst corresponding to a Pd amount of 1.5 mg and 60 ml of absolute ethanol were poured into a 80 ml four-necked stirring reactor, equipped with gassing stirrer and connections to a mercury-sealed precision gas burette and an argon/vacuum unit. The reactor was closed with a septum, evacuated and filled with H_2 several times. The suspension was equilibrated in the presence of H_2 at a temperature of 25 °C and a stirring speed of 2000 rpm for 10 min before 17 mmol of the substrate was injected through the septum via a syringe. The H_2 consumption was registered per minute. From the course of the H_2 consumption during the first 10 min of the reaction the activity of the catalyst was calculated in terms of ml(H_2)/g(Pd) min.

3. Results and discussion

3.1. Formation and characterisation of catalysts

In all experiments either 2.0 or 3.5 nm sized $(n\text{-}C_8H_{17})_4N^+Br^-$-stabilised Pd colloids [5] and NaF as a basic catalyst were used in the sol–gel experiments. Upon hydrolysing $Si(OCH_3)_4$ or $CH_3Si(OCH_3)_3$ in the presence of the Pd colloids, entrapment with formation of gels having promising morphological properties was indeed observed (table 1, catalysts I and II). However, undesired cluster agglomeration (100–200 nm Pd particles) occurred consistently, irrespective of the conditions used (figure 2(a)). In the case of $Si(OCH_3)_4/(CH_3O)_3SiOAl(O$*sec*-$C_4H_9)_2$[3] as the gel precursors, no cluster agglomeration was detected, but the material turned out to be non-porous (table 1, catalyst III). In contrast, upon using $CH_3Si(OCH_3)_3/Mg(OC_2H_5)_2$ as the gel precursors, efficient encapsulation without particle agglomeration was achieved *as well as* formation of porous materials (table 1, catalysts IV–IX). Different catalysts were prepared in which the ratio of $CH_3Si(OCH_3)_3$ to $Mg(OC_2H_5)_2$ was varied. The TEM image of a typical sample shows that the material contains individual Pd clusters (figure 2(b)). Using shadow casting and ultramicrotomic techniques in combination with TEM, it was confirmed that the Pd nanoparticles are indeed embedded in the oxide matrix and not just bound to the outer surface. Physisorption measurements indicate that the oxide matrix itself is of mixed micro- and mesoporosity. In the case of the material made from $CH_3Si(OCH_3)_3/Mg(OC_2H_5)_2$ (2 : 1), the specific pore volume amounts to 0.198 cm^3/g and the specific surface area to 420 m^2/g (table 1, catalyst V). The use of less $Mg(OC_2H_5)_2$ (Si/Mg = 7 : 1) leads to an increase in specific pore volume (1.031 cm^3/g) and a slight decrease in specific surface area (282 m^2/g) (table 1, catalyst IX).

The hydrophobic catalysts II and IV–IX were also characterised by ^{13}C- and ^{29}Si-CP-MAS-NMR. Thus, the presence of methyl groups in the metal oxide matrix was un-

---

[3] $(CH_3O)_3SiOAl(O$*sec*-$C_4H_9)_2$ (dynasil) is commercially available.

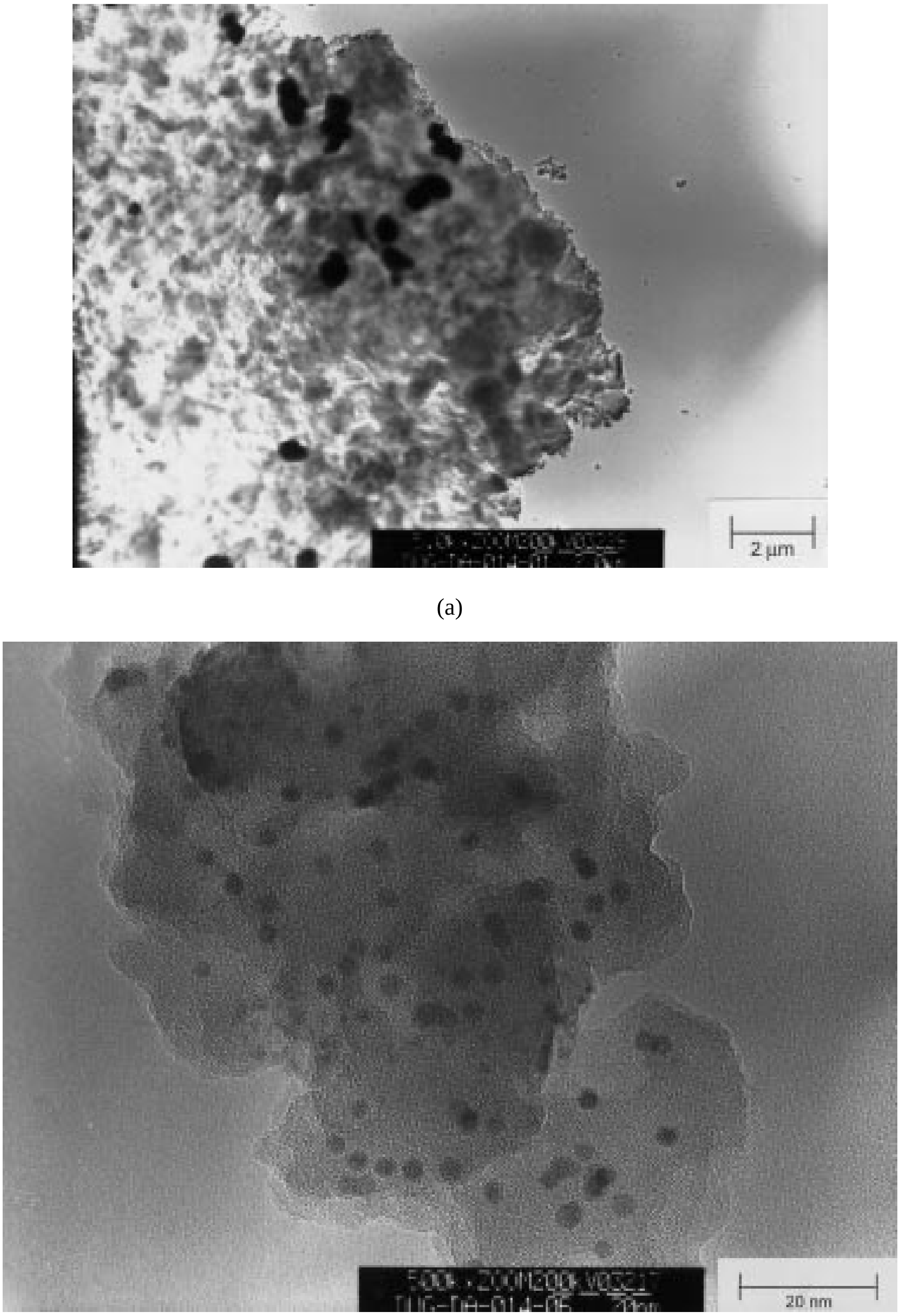

(a)

(b)

Figure 2. (a) TEM micrograph of a sol–gel material (catalyst II) prepared from $CH_3Si(OCH_3)_3$ and $(n\text{-}C_8H_{17})_4N^+Br^-$-stabilised Pd colloids (3.5 nm). (b) TEM micrograph of a Pd containing sol–gel material (catalyst VI) prepared from $CH_3Si(OCH_3)_3/Mg(OC_2H_5)_2$ (3 : 1) and $(n\text{-}C_8H_{17})_4N^+Br^-$-stabilised Pd colloids (3.5 nm).

ambiguously demonstrated (^{13}C-NMR signal at -3.4 ppm). On the basis of the ^{29}Si-NMR patterns the degree of Si–O–Si crosslinking was determined to be 89 and 92% in the case of catalysts VII and IX, respectively. It was not possible to measure the degree of Si–O–Mg crosslinking by this technique.

The X-ray powder diffraction (XRD) pattern of a typical Pd immobilisate (catalyst IX) clearly reveals the amorphous

Table 2
Characterisation of select Pd catalysts by elemental analysis, CO chemisorption and hydrophobicity measurements.

Catalyst	Pd[a] (wt%)	P dispersion[b] (%)	Hydrophobicity index
V	1.82	28.4	0.86
VII	1.90	39.2	1.63
IX	2.01	54.2	2.01
X	5	36.0	0.59

[a] From elemental analysis.
[b] Derived from CO-chemisorption measurements. The stoichiometric factor (CO/Pd) was assumed to be 0.75.

character of the sol–gel matrix. The presence of crystalline Pd particles is indicated by a broad peak at 2θ of 39°, also implying a crystallite size of a few nanometers.

In further experiments FTIR spectroscopy based on diffuse reflectance (DRIFTS) [17] after adsorption of pyridine was used to determine the surface acidity of the hydrophobic silica/magnesia mixed oxides (catalysts IV–IX). In the spectra the region of 1540 cm^{-1} is attributed to the pyridinium ion formed by the interaction with Brønsted acidic sites, whereas Lewis sites are indicated by absorption at 1605, 1580 and 1450 cm^{-1} and nonacidic silanol groups by signals at 1450 (overlap with Lewis site absorption) and 1595 cm^{-1}. Although Brønsted acidity might be expected, the materials display only a weak Lewis acidity which can be seen from the spectra where the typical absorption of Brønsted sites is absent.

Finally, the dispersion of the Pd particles of select catalysts as measured by CO chemisorption and the hydrophobicity index [14,15] as derived by the relative adsorption of H_2O and n-octane were determined (table 2). In contrast to conventional Pd/Al_2O_3 (catalyst X), the methyl-modified Si/Mg mixed oxides containing the Pd clusters are clearly hydrophobic (e.g., catalysts V, VII and IX).

3.2. Applications in catalysis

In order to test the catalytic properties of the various catalysts, the hydrogenation of 1,5-cyclooctadiene (**1**) with formation of cyclooctene (**2**) as the main product and cyclooctane (**3**) as the side product was chosen as the model reaction:

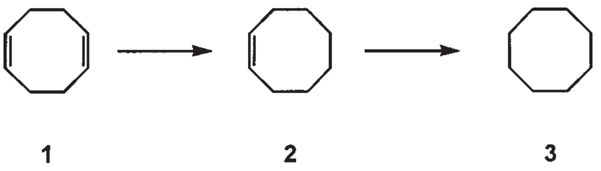

For the purpose of comparison, commercially available Pd/Al_2O_3 (catalyst X) was included in this exploratory study.

Table 3
Activity measurements of the Pd sol–gel catalysts and a commercial Pd/Al_2O_3 catalyst in the hydrogenation of 1,5-cyclooctadiene (**1**) as measured in terms of $\mathrm{ml(H_2)/g(Pd)\,min}$.

Catalyst	Catalyst activity
I	2500
II	2600
III	0
IV	5300
V	6800
VI	10100
VII	10600
VIII	13500
IX	13900
X	8800

Table 4
Dependency of the hydrogenation activity of two Pd sol–gel catalysts and a commericial Pd/Al_2O_3 catalyst as a function of particle (grain) size.

Catalyst	Particle size range[a] (μm)	Activity[b]
V	20–40	9500
	63–100	8600
	100–200	6300
IX	20–40	13800
	63–100	13800
	100–200	12900
X	20–40	10300
	40–63	8900
	100–200	6800

[a] Different particle (grain) size ranges were obtained by sieving the catalyst powders with a RETSCH VS 1000 sieve machine.
[b] Catalytic activity was measured in terms of $\mathrm{ml(H_2)/g(Pd)\,min}$ in the hydrogenation of **1**.

Table 3 shows some clear trends. The poor performance of the catalyst lacking any activity (catalyst III) can readily be explained by its extremely low porosity, although no agglomeration of the nanosized Pd particles has occurred. Somewhat higher activities are observed in the case of micro–mesoporous materials having higher specific pore volumes (catalysts I and II). However, the increase in activity is limited due to the fact that serious particle agglomeration has occurred. Indeed, these two catalysts are considerably less active than commercial Pd/Al_2O_3 (catalyst X). In contrast, the family of materials based on $CH_3Si(OCH_3)_3/Mg(OC_2H_5)_2$ constitutes an active class of catalysts (tables 1 and 3, catalysts IV–IX). They all have in common relatively high specific pore volumes *as well as* individual cluster entrapment. The most active gel (catalyst IX) is considerably more active than commercial Pd/Al_2O_3 (catalyst X). In both cases selectivity for cyclooctene (**2**) was found to be 93%. The differences in catalyst activity within this family of materials are essentially independent of the Pd particle size within the range of 2–3.5 nm (table 3, catalyst VI versus VII). Rather, they can be traced to differences in specific pore volumes. The higher the specific pore volume, the higher the activity. This is probably due to the improved accessibility of the entrapped Pd particles, which raises the question of diffusion limitation.

In order to study possible pore diffusion control, the effect of particle size [18] (grain size) of several of the solid materials was ascertained (table 4). In the case of the catalyst derived from $CH_3Si(OCH_3)_3/Mg(OC_2H_5)_2$ (2 : 1) (table 4, catalyst V), catalyst activity increases with decreasing particle (grain) size, indicating pore diffusion limitation. In contrast, essentially no effect is observed in the case of the similar catalyst having a significantly larger specific pore volume (table 4, catalyst IX). Obviously, in this case there is no pore diffusion limitation in the model reaction involving this particular catalyst. For comparison, the behaviour of commercial Pd/Al_2O_3 (catalyst X) was also studied. Accordingly, pore diffusion limitation was observed, inspite of the high porosity of the material. Different degrees of hydrophobicity of the oxide matrix may be the determining factor for the observed differences in activity, as has been observed in the case of entrapped enzymes in similar alkyl-modified sol–gel materials [13] and in alkyl-modified Si/Ti amorphous mixed oxides [14].

In summary, we have shown that it is possible to entrap preformed $R_4N^+Br^-$-stabilised Pd clusters in hydrophobic sol–gel materials formed from alkyl-modified silanes of the type $CH_3Si(OCH_3)_3$. This can be accomplished in such a way that individual Pd clusters are fixed in the sol–gel matrix without any signs of undesired agglomeration. The hydrophobicity of the matrix can be controlled by adjusting the amount of $CH_3Si(OCH_3)_3$ used with respect to the second component $Mg(OC_2H_5)_2$. It remains to be seen whether this new class of catalysts is useful in other reactions and whether bimetallic colloids can also be entrapped in such hydrophobic matrices.

Acknowledgement

We thank B. Tesche and B. Spliethoff for TEM measurements.

References

[1] (a) G. Schmid, ed., *Clusters and Colloids: From Theory to Applications* (VCH, Weinheim, 1994);
(b) J.H. Fendler, ed., *Nanoparticles and Nanostructured Films* (Wiley/VCH, Weinheim, 1998).

[2] M.T. Reetz, W. Helbig, S.A. Quaiser, U. Stimming, N. Breuer and R. Vogel, Science 267 (1995) 367.

[3] J.S. Bradley, in: *Clusters and Colloids: From Theory to Applications*, ed. G. Schmid (VCH, Weinheim, 1994) ch. 6.

[4] (a) T. Teranishi and M. Miyake, Chem. Mater. 10 (1998) 594;
(b) G.W. Busser, J.G. van Ommen and J.A. Lercher, in: *Adv. Catal. Nanostruct. Mater.*, ed. W.R. Moser (Academic Press, San Diego, 1996) p. 213;
(c) M. Antonietti, F. Gröhn, J. Hartmann and L. Bronstein, Angew. Chem. 109 (1997) 2170; Angew. Chem. Int. Ed. Engl. 36 (1997) 2080;
(d) M.P. Pileni, Ber. Bunsen-Ges. 101 (1997) 1578.

[5] (a) M.T. Reetz and W. Helbig, J. Am. Chem. Soc. 116 (1994) 7401;
(b) M.T. Reetz and S.A. Quaiser, Angew. Chem. 107 (1995) 2461; Angew. Chem. Int. Ed. Engl. 34 (1995) 2240.

[6] (a) D.G. Duff, T. Mallat, M. Schneider and A. Baiker, Appl. Catal. A 133 (1995) 133;
(b) L.M. Liz-Marzan, M. Giersig and P. Mulvaney, Langmuir 12 (1996) 4329;
(c) M.T. Reetz, S.A. Quaiser, R. Breinbauer and B. Tesche, Angew. Chem. 107 (1995) 2956; Angew. Chem. Int. Ed. Engl. 34 (1995) 2728;
(d) H. Bönnemann and W. Brijoux, in: *Adv. Catal. Nanostruct. Mater.*, ed. W.R. Moser (Academic Press, San Diego, 1996) p. 165.

[7] S. Kawi and B.C. Gates, in: *Clusters and Colloids: From Theory to Applications*, ed. G. Schmid (VCH, Weinheim, 1994) p. 299.

[8] (a) D.S. Shephard, T. Maschmeyer, B.F.G. Johnson, J.M. Thomas, G. Sankar, D. Ozkaya, W. Zhou, R.D. Oldroyd and R.G. Bell, Angew. Chem. 109 (1997) 2337; Angew. Chem. Int. Ed. Engl. 36 (1997) 2242;
(b) D.S. Shephard, T. Maschmeyer, G. Sankar, J.M. Thomas, D. Ozkaya, B.F.G. Johnson, R. Raja, R.D. Oldroyd and R.G. Bell, Chem. Eur. J. 4 (1998) 1214.

[9] U. Junges, F. Schüth, G. Schmid, Y. Uchida and R. Schlögl, Ber. Bunsen-Ges. 101 (1997) 1631.

[10] A. Martino, S.A. Yamanaka, J.S. Kawola and D.A. Loy, Chem. Mater. 9 (1997) 423.

[11] M.T. Reetz, W. Helbig and S.A. Quaiser, Patent EP 0 672 765 A1 (1995).

[12] M. Dugal, Diplomarbeit, Universität Duisburg (1996).

[13] (a) M.T. Reetz, A. Zonta and J. Simpelkamp, Angew. Chem. 107 (1995) 373; Angew. Chem. Int. Ed. Engl. 34 (1995) 301;
(b) M.T. Reetz, Adv. Mater. 9 (1997) 943.

[14] S. Klein and W.F. Maier, Angew. Chem. 108 (1996) 2376; Angew. Chem. Int. Ed. Engl. 35 (1996) 2230.

[15] C.H. Berke, A. Kiss, P. Kleinschmit and J. Weitkamp, Chem. Ing. Tech. 63 (1991) 623.

[16] (a) K. Kaneda, M. Higuchi and T. Imanaka, J. Mol. Catal. 63 (1990) L33;
(b) R.L. Augustine and S.T. O'Leary, J. Mol. Catal. A 95 (1995) 277.

[17] K. Tanabe, in: *Catal. Sci. Technol.*, Vol. 2, eds. J.R. Anderson and M. Boudart (Springer, Berlin, 1981) ch. 5.

[18] V. Ponec and G.C. Bond, *Catalysis by Metals and Alloys*, Stud. Surf. Sci. Catal., Vol. 95 (Elsevier, Amsterdam, 1995).